

Lamprophyres from Abu Rusheid-Sikait Area, South Eastern Desert, Egypt: Rare Earth Elements, Mineralization and Spectrometric Prospecting

Gehad M. Saleh^{1*}, Hanaa A. El Dokouny², Maher I. Dawoud² and Samir M. Sabry²

¹Nuclear Materials Authority, P.O. Box 530, El-Maadi, Cairo, Egypt

²Geology Department, Faculty of Science, Minufiya University, Egypt

***Corresponding Author:** Gehad M. Saleh, Nuclear Materials Authority, P.O. Box 530, El-Maadi, Cairo, Egypt

Abstract: Wadi Abu Rusheid - Wadi Sikait area lies in the southern part of the Eastern Desert of Egypt. It is located about 40 km west of the Red Sea coast, along Wadi Nugrus which is a tributary of Wadi El Gemal. The surrounding area of lamprophyre dykes comprises, ophiolitic mélangé, cataclastic (mylonitic) rocks, granitic rocks and post granitic dykes and veins. The lamprophyre dyke is intruding in the shear zone along the mylonitic rocks. This shear zone varies in thickness from 0.5 m to 2.0 m and up to 1.0 km long. The alteration is represented by the sericitization and argilization, as well as hematitization.

Petrographically, it is composed mainly of plagioclases phenocrysts embedded in fine-grained groundmass of plagioclase, ferromagnesian minerals and quartz. U-minerals, apatite and opaques are accessory. The mylonitic rock consists essentially of quartz, K-feldspars, plagioclases, biotite and muscovite. Zircon, xenotime, monazite, allanite, fluorite and opaques are accessories.

The mineralizations of the mylonitic rocks and lamprophyre dykes at the studied area can be classified on basis of mode of occurrence and lithological associations into: -1) Uranium minerals (kasolite), 2) Base metals minerals (sphalerite - cerussite) and 3) REE and Niobium - Tantalum bearing minerals (xenotime - monazite - tantalite - fergusonite - allanite - apatite - zircon).

Geochemically, the studied lamprophyre dykes are characterized by anomalously high REEs contents ranging from 1035 to 3980 ppm. The LRREs are about 200 to 1000 times the normalized chondritic values while the HREEs recorded values about 700 to 5000 times compared to the reference chondrite (HREEs>LREEs). The geochemical investigations indicate the REE patterns of the lamprophyres dykes in Wadi Abu Rusheid - Wadi Sikait area show HREE enrichment and strong Eu negative anomalies. The presence of REE-rich hydrothermal phases suggests a significant mobilization and deposition of REEs, especially La, Pr, and Sm (LREE) and Gd, Tb, Dy, Ho, Er, Tm, Yb and Lu (HREE).

Radiometrically, there are relatively positive relation between eU vs. eTh , slightly strong positive relation between eU vs. $K\%$, eU vs. eU/eTh and weakly positive relation between eTh vs. $K\%$. These positive values of eU indicating the migration of uranium and redeposit in lamprophyre dykes, leading to the enrichment of uranium in lamprophyre dykes from surrounding rocks and enrichment in uranium which related to post-magmatic processes.

Keywords: Rare earth elements, Uranium and zinc minerals, Spectrometric prospecting, Lamprophyre dykes, Abu Rusheid-Sikait Area, Egypt.

1. INTRODUCTION

Abu Rusheid - Sikait area has attracted many authors (Hassan, 1964 and 1973, Saleh, 1997, Assaf et al., 2000, El Ghazalawi, 2009 and Ibrahim et al., 2004, 2006 and 2010). Abu Rusheid area comprises ophiolitic mélangé and cataclastic (mylonitic) rocks. These rocks associations are intruded by younger granitic rocks. Abu Rusheid cataclastic (mylonitic) rocks are cut by lamprophyre dykes in NNW-SSE and ENE-WSW directions. The NNW-SSE lamprophyre is considered as good trap for poly-mineralization (Ibrahim et al., 2006). Gold, tungsten - sulfide, galena and pyrite are recorded in Wadi Sikait (Ibrahim et al., 1999). The present study is concerned with detailed petrography, mineralogy, rare earth elements (REEs) geochemistry and spectrometric prospecting of the lamprophyre dykes, South Eastern Desert, Egypt.

2. GEOLOGIC SETTING AND PETROGRAPHY

2.1. Regional Geology of Abu Rusheid Area

Abu Rusheid-Sikait area located at about 90 km SW from Marsa Alam City, South Eastern Desert and is accessible from the Red Sea through Wadi El-Gemal Desert track. The TM image of band ratios covers a major part of study area (Fig.1) was used in regional interpretation for general rock types identification and association. Abu Rusheid-Sikait area is bordering to the major shear zone known as the Nugrus thrust fault (Saleh, 1997, Greiling et al., 1988) or the Nugrus strike-slip fault (Fritz et al., 1996) and or Ras Shait-Nugrus shear zone (Fowler and Osman, 2009). This shear zone separates high-temperature metamorphic rocks of the Hafafit complex in the SW from mainly low-grade ophiolitic and arc volcanic assemblages known as Ghadir group to the NE. The Nugrus major thrust runs along the upper part of W. Sikait in a NW direction till the southern tip of Gabal Ras Shait, then swings to a south westward direction along W. Shait west of G. Migif. The Migif-Hafafit gneisses comprise the foot wall of the Nugrus thrust, while the Ghadir group comprises its hanging wall (Saleh, 1997, El Bayoumi, 1984).

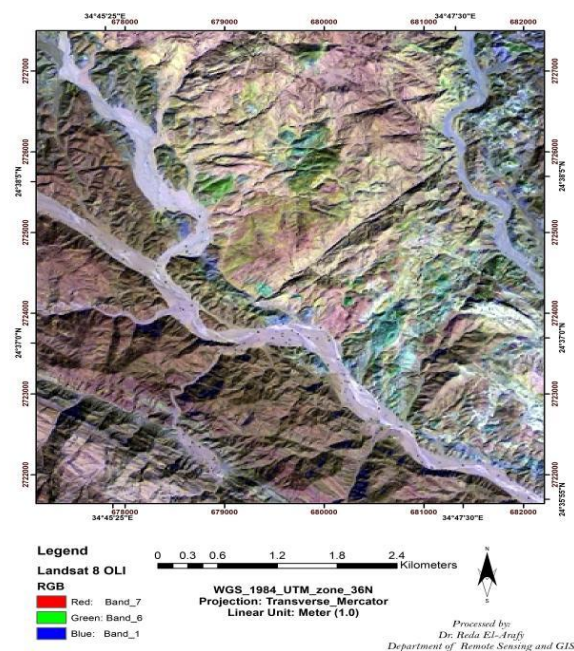


Fig.1 Landsat TM-Image of Abu Rusheid - Sikait area, South Eastern Desert, Egypt

The area of W. Nugrus, W. Abu Rusheid and W. Sikait comprises two napes (ophiolite rocks and arc assemblage), separated by ophiolitic mélangé (Fig. 2). These rocks associations are intruded by intracratonic gabbroic and granitic rocks (Saleh, 1997). These rocks are subjected to polycyclic deformation and characterized by regional WNW-ESE thrusting. Such thrusting is assigned to an age between 682 Ma (the time of emplacement of the older granitoids) and 565 to 600 Ma, the time of intrusion of the younger granites (Stern and Hedge, 1985). The rocks are generally intensively deformed and show clear gradual variation from low grade green schist facies, (Attawiya et al. 1989 and Surour, 1995) through the medium grade amphibolite facies (Staurolite - Kyanite - Silliminite facies). The dismembered ophiolite is mainly constituted of meta-peridotites, meta-pyroxenites, layered metagabbros and ortho-amphibolites (Saleh, 1997). The arc assemblage is constituted of metasediments (meta-calcpelites and meta-psammopelites), arc metavolcanics (meta-andesites and meta-dacites), and arc plutonites (diorites and quartz diorites). Abu Rusheid - Sikait granitic pluton elongated in NW-SE (12 km in long) and thinning in NE-SW (3 km in width). The granitic rocks are represented from the NW direction by porphyritic biotite granites and two mica granites, whereas the muscovite granites occupy the SE part of the pluton (Ibrahim et al. 2004).

2.2. Detailed Geology of Abu Rusheid Area

The detailed geologic map of the study area (3.0 km²) is characterized by low to moderate topography. The Precambrian rocks unit of the studied area (Fig. 3) are arranged as follows:

(a) ophiolitic mélange, consisting of ultramafic rocks and metagabbros set in metasediment matrix, (b) cataclastic (mylonitic) rocks, consisting of protomylonites, mylonites, ultramylonites and silicified ultramylonites (c) mylonitic granites (d) post-granite dykes and veins (Ibrahim et al., 2004).

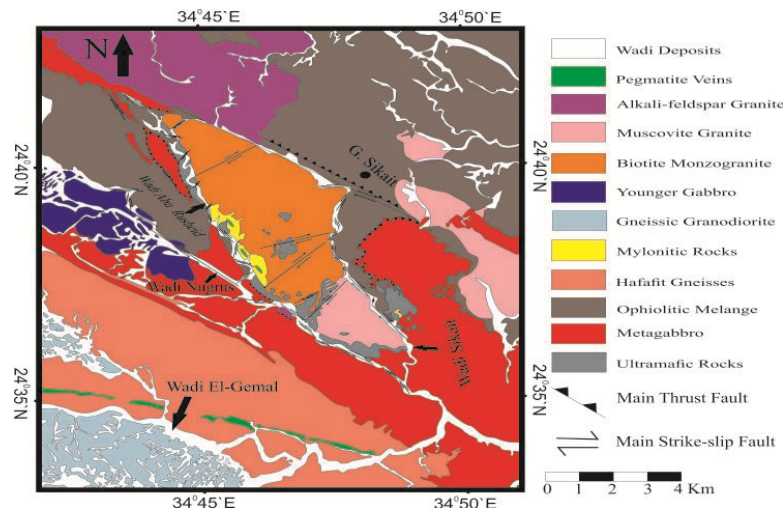


Fig.2 Regional geological map of Abu Rusheid – Sikait area, South Eastern Desert, Egypt (modified after Saleh, 1997)

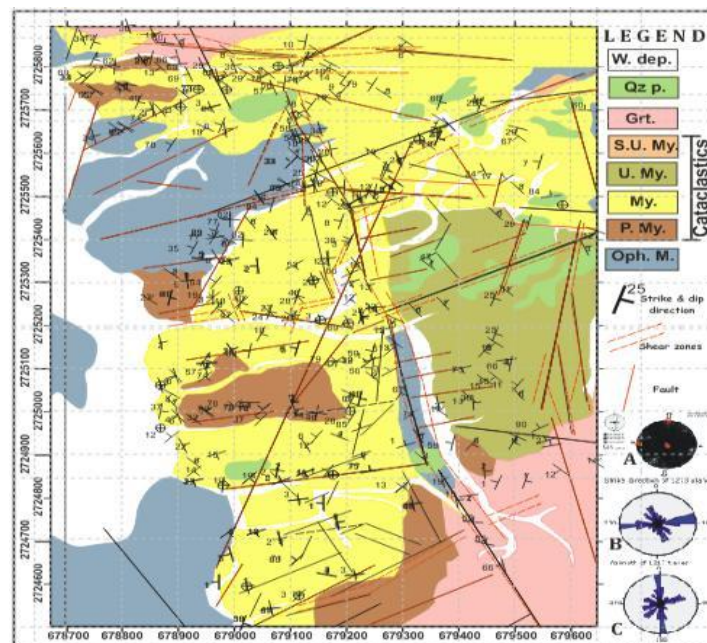


Fig.3 Detailed geologic map of Abu Rusheid area, South Eastern Desert, Egypt, Ibrahim et al. (2004), showing the structural lines as well as the investigated sites and the different rock types constitute (Saleh et al., 2012). (Oph. M.= ophiolitic mélange, My.= cataclastic, P.= proto, U.= ultra, S.= silicified, Grt.= granite, Qz.= quartz and W.dep.= Wadi deposits). A=lower hemisphere stereographic projection of fractures and the inferred stress tensor, B= rose diagram for fracture strikes and C= orientations of the induced (σ_3) axes.

2.2.1. Geology of Cataclastic (mylonitic) Rocks

W. Abu Rusheid - W. Nugrus cataclastic (mylonitic) rocks are exposed mainly at eastern side of W. Abu Rusheid extend to south Madinet Nugrus, covering about 3.0 km². These rocks are overthrust by ophiolitic mélange (Fig. 4a). They are intercalated with ophiolitic mélange and intruded together by biotite granites and crosscut by NE-SW and N-S strike slip faults. They are grey in colour, fine to medium-grained, exhibit gneissosity structures and usually are dissected by pegmatite and quartz veins, concordant with the vertical joints (Fig. 4b). These cataclastic (mylonitic) rocks are sometimes in reddish to yellowish staining of iron oxides. Columbite occurs abundantly as disseminated grains or as single dark crystal and aggregates visible by naked eyes (Ibrahim et al., 2004).

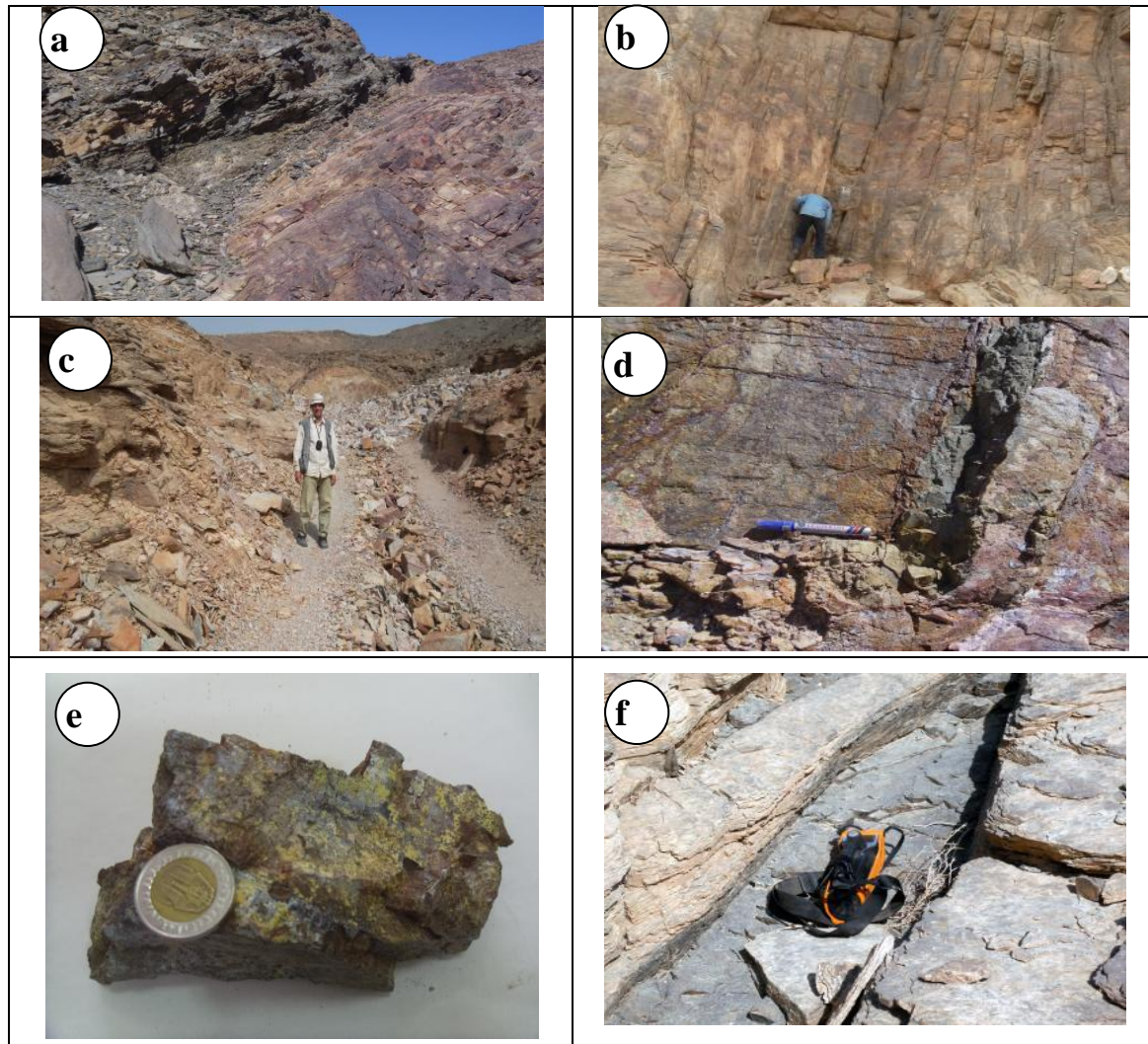


Fig.4 View showing:- a) ophiolitic *mélangé* thrust over the mylonitic rocks, b) vertical joints in mylonitic rocks, c) shear zone in mylonitic rocks, d) lamprophyre dykes dissected by dextral strike slip faults and highly fractured, e) visible uranium and zinc mineralizations in lamprophyre dykes and f) lamprophyre dyke cutting mylonitic rocks, South W. Abu Rusheid (Madinat Nugrus) area, Abu Rusheid area, SED, Egypt.

2.2.2. Abu Rusheid Post Granitic Dykes and Veins

The basement rocks of Abu Rusheid area cut by various dykes and veins. They comprise the following rocks types encountered in the mylonitic rocks:

2.2.2.1. Lamprophyre dykes

Abu Rusheid area is extruded by lamprophyre dykes, the direction, NNW-SSE and ENE-WSW. These dykes are fine-grained, altered and dark in colour. The NNW-SSE lamprophyre dykes vary in thickness from 0.5 m to 2.0 m and up to 1.0 km long cutting the mylonitic rocks and parallel to the shear zone, (Fig. 4c). The lamprophyre dyke dissected by sinistral and dextral strike slip faults and highly fractured (Fig. 4d). Visible uranium and zinc minerals are observed (Figs. 4e). The lamprophyre dyke in Madinat Nugrus area is discontinuous, varying in width from 0.5 m to 1.5 m and reaching up to 2.0 km in long (Fig. 4f).

2.3. Petrography

2.3.1. Lamprophyre dykes

Macroscopically, the lamprophyre dyke is fine-grained, porphyritic, highly altered and highly stained by iron oxides, giving red to yellow and brown colours. Microscopically, it is composed mainly of plagioclases ($An_{35} - 40$) phenocrysts embedded in fine-grained groundmass of plagioclase, ferromagnesian minerals and quartz. Opaques and apatite are accessory (Figs. 5 a, b and c).

Carbonates, secondary uranium minerals (kasolite) occur as radial crystals coated by REEs elements and opaques are secondary minerals.

2.3.2. . Cataclastic (mylonitic) rocks

Macroscopically, the mylonitic rock is fine to medium-grained, massive and altered. Microscopically, the rock consists essentially of quartz, K-feldspars, plagioclases (An_{10-18}), biotite and muscovite. Zircon, xenotime, monazite, allanite, fluorite and opaques are accessories (Figs. 5 d, e and f).

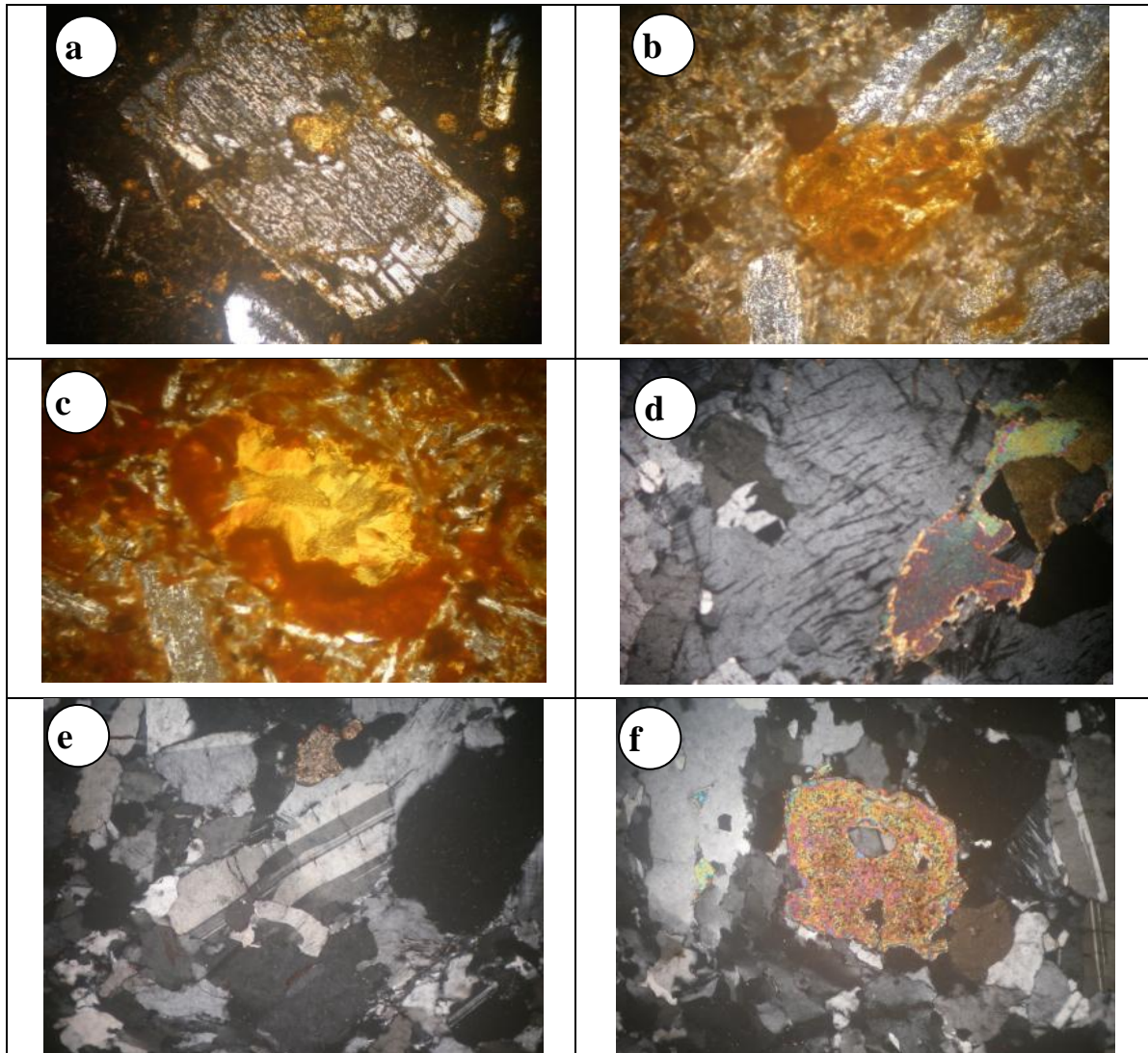


Fig.5 Photomicrograph showing:- a) plagioclase as fine laths in the groundmass and ferromagnesian minerals, lamprophyre dykes, (C.N., $X= 20$), b) opaques minerals occur as irregular grains to the groundmass of plagioclase or within clinopyroxene, sometimes show the red colour due to presence of iron oxy-hydroxides, lamprophyre dykes, (C.N., $X= 20$), c) secondary uranium minerals are represented as radiated uranium minerals filling ocelli texture of carbonates in core followed by REEs elements and iron oxides, lamprophyre dykes, (C.N., $X= 20$), d) k-feldspars are represented by perthite which are euhedral crystals, mylonitic rocks, (C.N., $X= 20$), and e) plagioclases and have inclusions of zircon, mylonitic rocks, and f) zircon occurs as euhedral prismatic crystals and associated with plagioclase, mylonitic rocks, Abu Rusheid area, SED, Egypt, (C.N., $X= 20$).

3. MINERALIZATIONS

The mineralizations of the mylonitic rocks and lamprophyre dykes at the studied area can be classified on basis of mode of occurrence and lithological associations into:- 1) Uranium minerals (kasolite), 2) Base metals minerals (sphalerite - cerussite) and 3) REE and Niobium - Tantalum bearing minerals (xenotime - monazite - tantalite - fergusonite - allanite - apatite - zircon).

3.1. Uranium Minerals

3.1.1. Kasolite

Kasolite ($Pb(UO_2)SiO_4 \cdot H_2O$) was originally determined by (Huyneq et al., 1963), consisting of a hydrous uranium lead silicate. The kasolite structure is very closely related to the structure of boltwoodite (Heinrich, 1962). Kasolite generally occurs either as minute dispersions or microfractures infilling and coatings on surfaces of hematized joints. Kasolite is found in the lamprophyre dykes and is confirmed by ESEM techniques and contains 56.61% U, 28.69% Pb and 8.64% Si (Fig. 6a).

3.2. Base metals minerals

3.2.1. Sphalerite

Sphalerite ZnS is a cubic crystal. It is a brittle mineral with hardness ranges from 3.5 to 4. It is transparent to translucent, opaque when iron-rich with highly variable colours ranging from colourless to dark brown, black colour. Sphalerite is associated with galena, chalcopyrite, marcasite, pyrite and fluorite (Heinrich, 1962). It is found in lamprophyre dykes and is confirmed by ESEM techniques and contains 38.14.37% S, 61.19.80% Zn and 0.67% Fe (Fig. 6b).

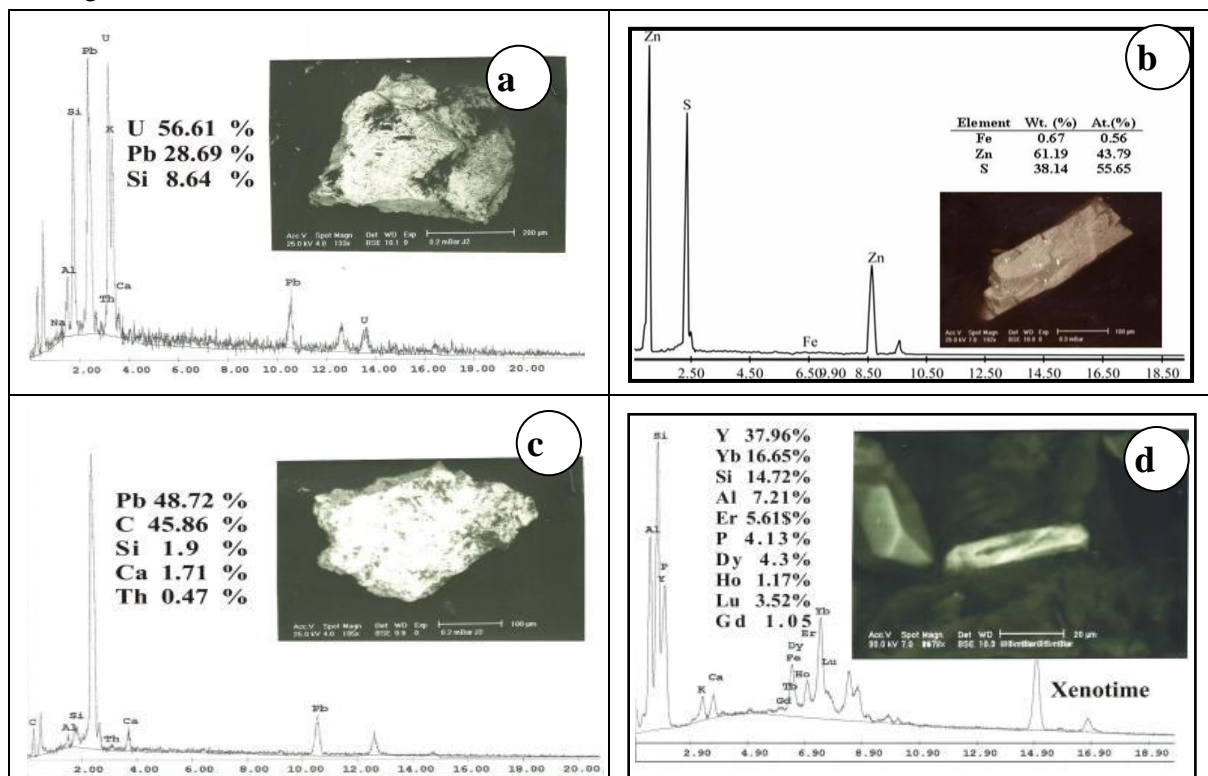
3.2.2. Cerussite

Cerussite (also known as lead carbonate or white lead ore) is a mineral consisting of lead carbonate ($PbCO_3$), and an important ore of lead. Cerussite crystallizes in the orthorhombic system and is isomorphous with aragonite (Heinrich, 1962). It has a Mohs hardness of 3 to 3.75 and a specific gravity of 6.5. It is found in lamprophyre dykes and is confirmed by ESEM techniques and contains 48.72% Pb, 45.86% C, 1.9% Si, 1.71% C and 0.47% Th (Fig. 6c).

3.3. REE and Niobium - Tantalum bearing minerals

3.3.1. Xenotime

Xenotime (YPO_4) is a rare earth phosphate mineral, whose major component is yttrium phosphate, rare earth elements particularly erbium and cerium, may substitute for Y, Th, U, Zr and Ca also substitute for Y in small amounts (Palache et al., 1951 and Heinrich, 1962). Xenotime is prismatic in habit with pyramidal terminations and greenish colour. The ESEM techniques detected the presence of xenotime that contains 37.96% Y, 16.65% Yb, 5.62% Er, 4.13% P, 4.3% Dy, 1.05% Gd and 3.52% Lu (Fig. 6d).



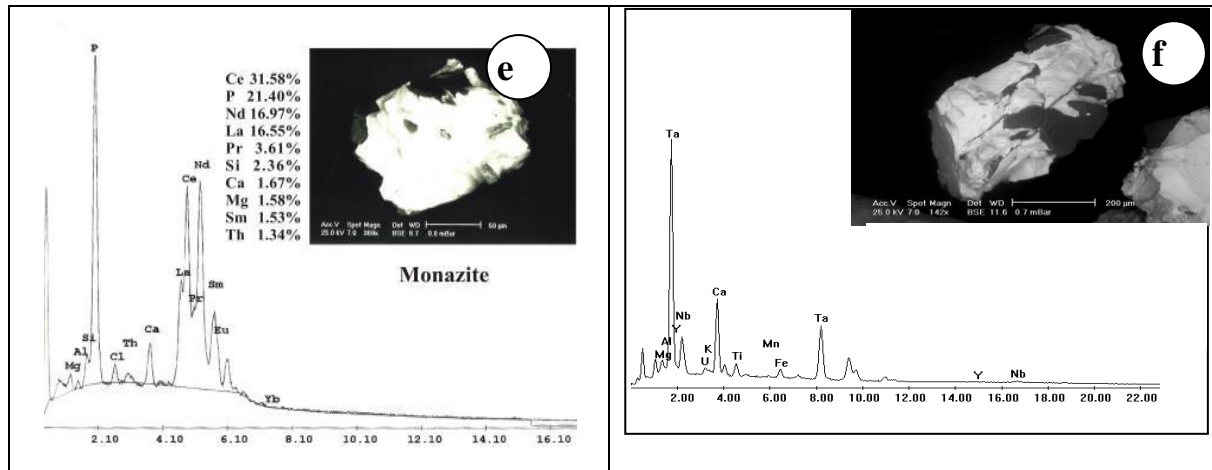


Fig.6 ESEM image and EDX analysis data of:- a) kasolite mineral, b) sphalerite mineral, c) cerussite mineral, d) xenotime mineral, e) monazite mineral, and f) tantalite mineral of the studied lamprophyre dykes, Southeastern Desert, Egypt.

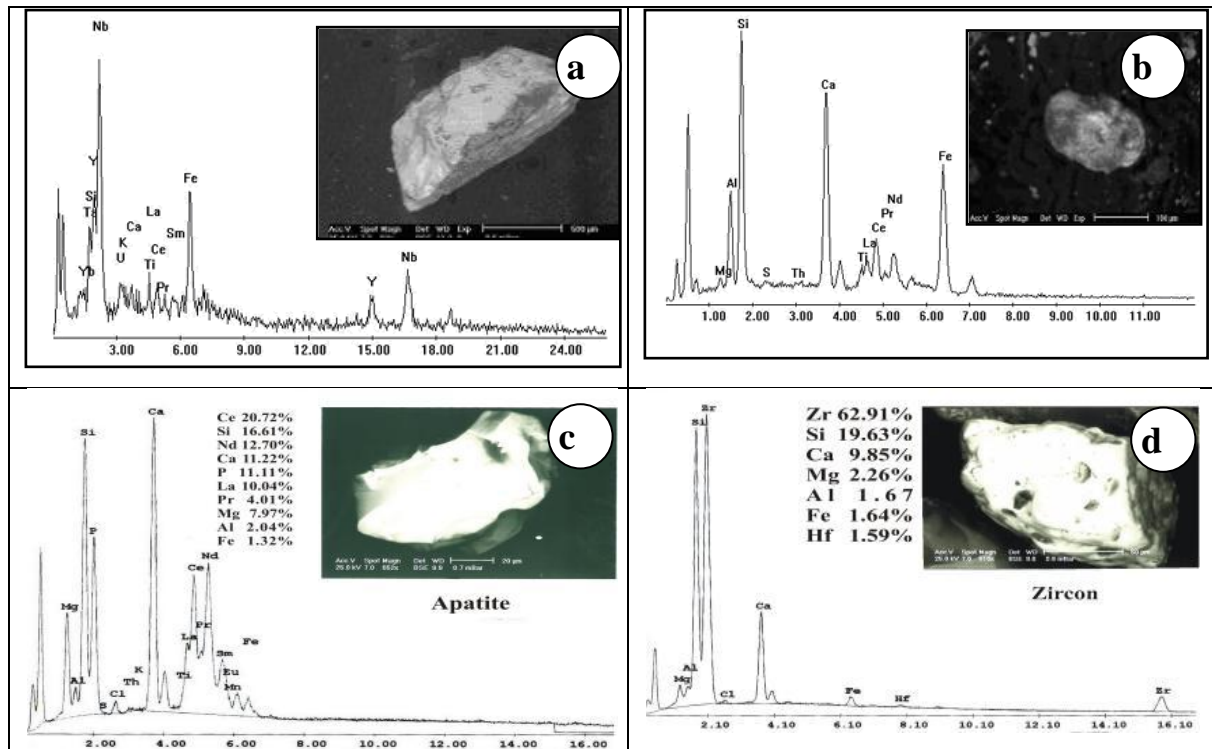


Fig.7 ESEM image and EDX analysis data of:- a) fergusonite mineral, b) allanite mineral, c) apatite mineral, and d) zircon mineral of the studied lamprophyre dykes, South Eastern Desert, Egypt.

3.3.2. Monazite

Monazite $(Ce,La,Nd,Th)(PO_4.SiO_4)$ is a rare earth phosphate with appreciable substitution of thorium for rare earth and silicon for phosphorous (Heinrich, 1962). This mineral can be considered as LREEs-bearing minerals, especially Ce. The ESEM techniques detected the presence of monazite that contains 31.58% Ce, 21.40% P, 16.55% La, 3.61% Pr and 1.53% Sm (Fig. 6e).

3.3.3. Tantalite

Tantalite $(Fe,Mn)(Ta,Nb)_2O_6$ has been recorded in the Abu Rusheid - Sikait area. It belongs to columbite-tantalite series. Most crystals are stained with iron oxide which are partially coated grains or coated all surface of grains (Heinrich, 1962). Tantalite occurs as black to deep brown with metallic appearance, prismatic and euhedral to subhedral crystals and confirmed by SEM and contains 65.5 Ta %, 10.44 Nb %, 11.55 % Ca, 4.84 U %, and 3.23 Y % (Fig. 6f).

3.3.4. *Fergusonite*

Fergusonite (Ce,La,Y)NbO₄ is a prismatic crystals and irregular poikiloblasts. Its hardness is from 5.5 to 6.5. Fergusonite is semitransparent, dark red to black, reddish colour. It is dimorphous with fergusonite-beta-(Ce). Fergusonite is associated with pyrite, columbite, allanite, bastnäsité, and monazite (Heinrich, 1962). Fergusonite occurs in lamprophyre dykes and is confirmed by ESEM techniques (Fig. 7a).

3.3.5. *Allanite*

Allanite (Ca,Ce)₂(Al, Fe²⁺, Fe³⁺)₃(SiO₄)(OH) is a cerium-bearing epidote. In most cases allanite mineral is uranium and thorium carrier and altered to an amorphous substance product by breakdown of the space lattice by radioactive emanation ((Heinrich, 1962, Kerr, 1977 and Deer et al., 1992). The mineral is found in lamprophyre dykes and confirmed by ESEM techniques (Fig. 7b).

3.3.6. *Apatite*

Apatite Ca₅(PO₄)₃(OH,F,Cl) is a group of phosphate minerals. Apatite is the defining mineral for 5 on the Mohs scale. The intensity of the colour increases with an increase in Mn content of the apatite (Heinrich, 1962 and Deer et al., 1992). It contains 11.22% Ca, 20.72% Ce, 12.70% Nd and 11.11% P. It is confirmed by ESEM (Fig. 7c).

3.3.7. *Zircon*

Zircon ZrSiO₄ is tetragonal, most commonly as tabular to prismatic crystals. Deer et al., (1992), stated that rounding shape of zircon can take place in igneous rocks by magmatic adsorption and corrosion of the grains may be due to metasomatism. Fielding (1970), stated that the colour of zircon crystals may be associated with the presence of uranium. Pupin and Turcon (1975), Vavra (1990) and Dawoud, (2004) proposed that zircon shape is a function of the conditions or environment of crystallization. In particular, formation of the bipyramidal faces is related to the slow crystallization and substitution by U, Th, REE and P. It is confirmed by the ESEM techniques and contains 62.91% Zr, 19.63% Si and 1.91% Hf. It is found in the studied mylonitic rocks and lamprophyre dykes (Fig. 7d).

4. RARE EARTH ELEMENTS (REES) GEOCHEMISTRY

The REEs are the most useful of all trace elements and REEs studies have important applications in igneous, sedimentary and metamorphic petrology. REEs comprise atomic numbers 57 (La) to 71 (Lu). Promethium (61) is not found naturally. Yttrium (Y, 39) has an ionic charge of 3+, like that of REEs, and a radius (1.019 Å) similar to that of holmium (1.015 Å) and is, therefore, sometimes included as a REEs (Myron, 2003). The REEs are normally presented on concentration vs. atomic number diagram on which concentration are normalized on the chondritic reference value, expressed as the logarithm to the base 10 of the value. Concentrations at individual points on the graph are joined by straight lines. This is sometimes referred to as the Masuda-Coryell diagram after the original proponents of the diagram (Myron, 2003). Trends on REEs patterns are usually referred to as REEs "patterns" (Rollinson, 1993). Two properties of REEs make them especially useful as petrogenetic indicators: a) They are generally insoluble in aqueous fluids; hence, they are useful in altered or weathered rocks and b) Trivalent ions of REEs have decreasing radii with respect to increasing atomic number, from La (1.160 Å) to Lu (0.977 Å). Plagioclase, because of the similarity of Eu²⁺ to Ca²⁺, will accommodate much more of this trace element than immediately adjacent lighter and heavier trivalent REEs, creating a positive Eu anomaly. To smooth out the otherwise sawtoothlike absolute abundances of odd and even atomic numbers (the Oddo-Harkins effect), the concentration of a REEs in a rock is divided by the concentration of the same element in average chondritic meteorites. This sample/chondrite ratio is then plotted on a logarithmic scale (Myron, 2003). The trace elements and REE elements distribution illustrated in (Figs. 8 a and b) are; U (4%), Pb (44%), Cu (8%), Y (16%), Rb (3%), Zn (21%) and Zr (3%), La (7%), Ce (6%), Gd (4%), Er (18%), Dy (17%), Nd (11%), Yb (17%) and Sm (5%) and show anomalous concentrations in the studied lamprophyre dykes.

The normalized multi-element spider diagram for the studied rocks, using the normalizing values of primitive-mantle (Sun and McDonough, 1989 and McDonough et al., 1992), is shown in (Fig. 9). It is clear that enrichment in Rb, Th, Pb, Nd, Sm, Dy, Yb, Lu and depleted in Ba, K, Nb, Sr, Zr, Eu, Ti and

Y for the studied rocks. Such negative anomalies are related to following two processes; (a) contamination of the magma with crust that is depleted in these elements (Lightfoot, 1993) and (b) retention of these elements in the subduction zone sources of calc-alkaline magmas (Pearce, 1983).

The studied lamprophyre dykes are characterized by anomalously high REEs contents ranging from 1035 to 3980 ppm. The pattern relative to the values of the chondrite (after Boynton 1984), (Fig. 10) shows enriched heavy rare earth elements relative to the light rare earth elements. Nevertheless the LRREs are about 200 to 1000 times the normalized chondritic values while the HREEs recorded values about 700 to 5000 times compared to the reference chondrite (HREEs>LREEs). The REEs pattern is characterized by negative Ce and Nd troughs, where little positive spike of Pr is developed. Eu exhibits deeper negative anomaly which Eu/Eu^* ranges from 0.08 to 0.21. The lack of a Eu anomaly suggests that plagioclase fractionation (either by crystal fractionation or upper crustal contamination) was not important during the origin and differentiation of the original magma.

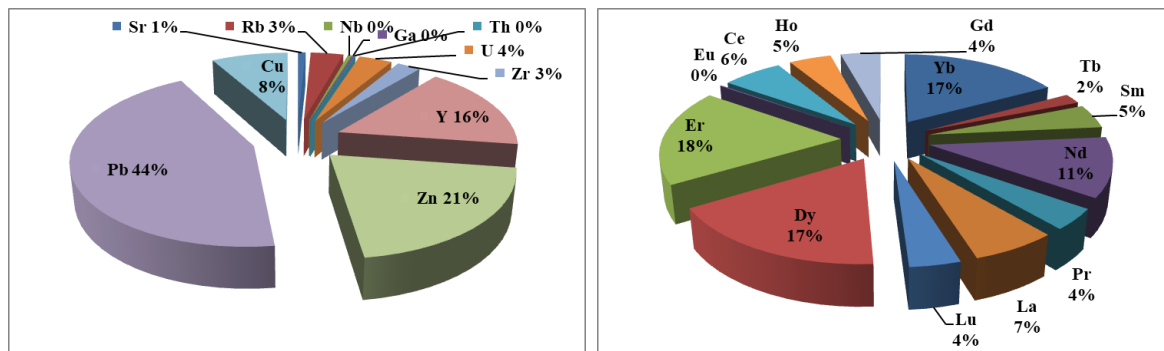


Fig.8 a): Pie-chart diagrams showing range of some trace elements and b) Pie-chart diagrams showing range of rare earth elements in the lamprophyre dykes of the studied area, South Eastern Desert, Egypt.

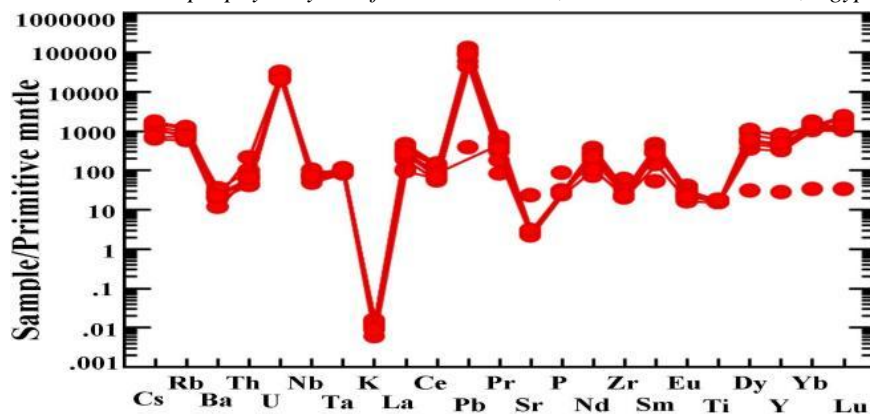


Fig.9 Primitive-mantle-normalized pattern of the studied lamprophyre dykes, South Eastern Desert, Egypt (Sun and McDonough, 1989 and McDonough et al., 1992)

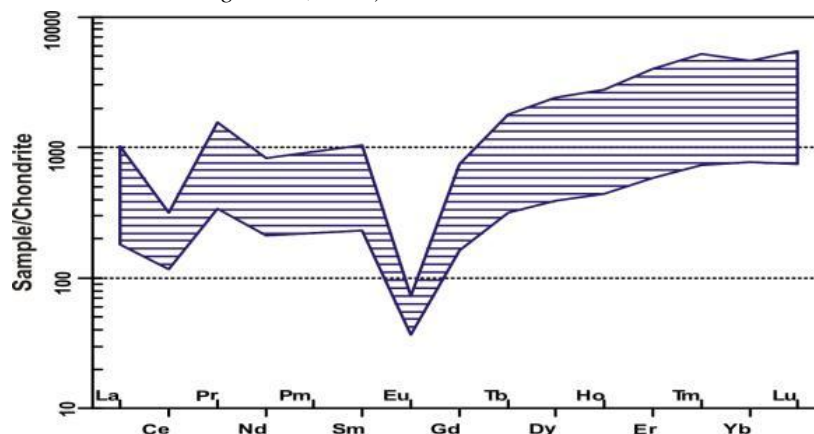


Fig.10 Chondrite-normalized patterns of the studied lamprophyre dykes, South Eastern Desert, Egypt (Boynton, 1984)

5. SPECTROMETRIC PROSPECTING

The field radiometric survey of W. Abu Rusheid - W. Sikait area has been executed using the hand-held differential spectrometer model "GS-256 and RS-230 gamma-ray spectrometer made by Geophysica LTD, Czechoslovakia which permit continuous monitoring and recording of any one of the four selected energy regions, Dose (mSvy-1) rate, TC, K, U and Th; or the sequential measurements of the four channels (Fig. 11).

Distribution of the radioelements in lamprophyre dykes in Abu Rusheid - Sikait area

The variation diagrams of the shear zones, mylonitic rocks and lamprophyre dykes at the Abu Rusheid - Sikait area (Figs. 12 and 13) showing that, there are relatively positive relation between eU vs. eTh, slightly strong positive relation between eU vs. K%, eU vs. eU/eTh and weakly positive relation between eTh vs. K%. These positive values of eU indicating the migration of uranium and redeposit in lamprophyre dykes and leading to the enrichment of uranium in lamprophyre dykes from surrounding rocks and enrichment in uranium which related to post-magmatic processes (Cambon,1994).



Fig.11 Multi-channel GS-256 portable spectrometer with gamma (γ) sensor (9903). Geophysica, LTD Czechoslovakia.

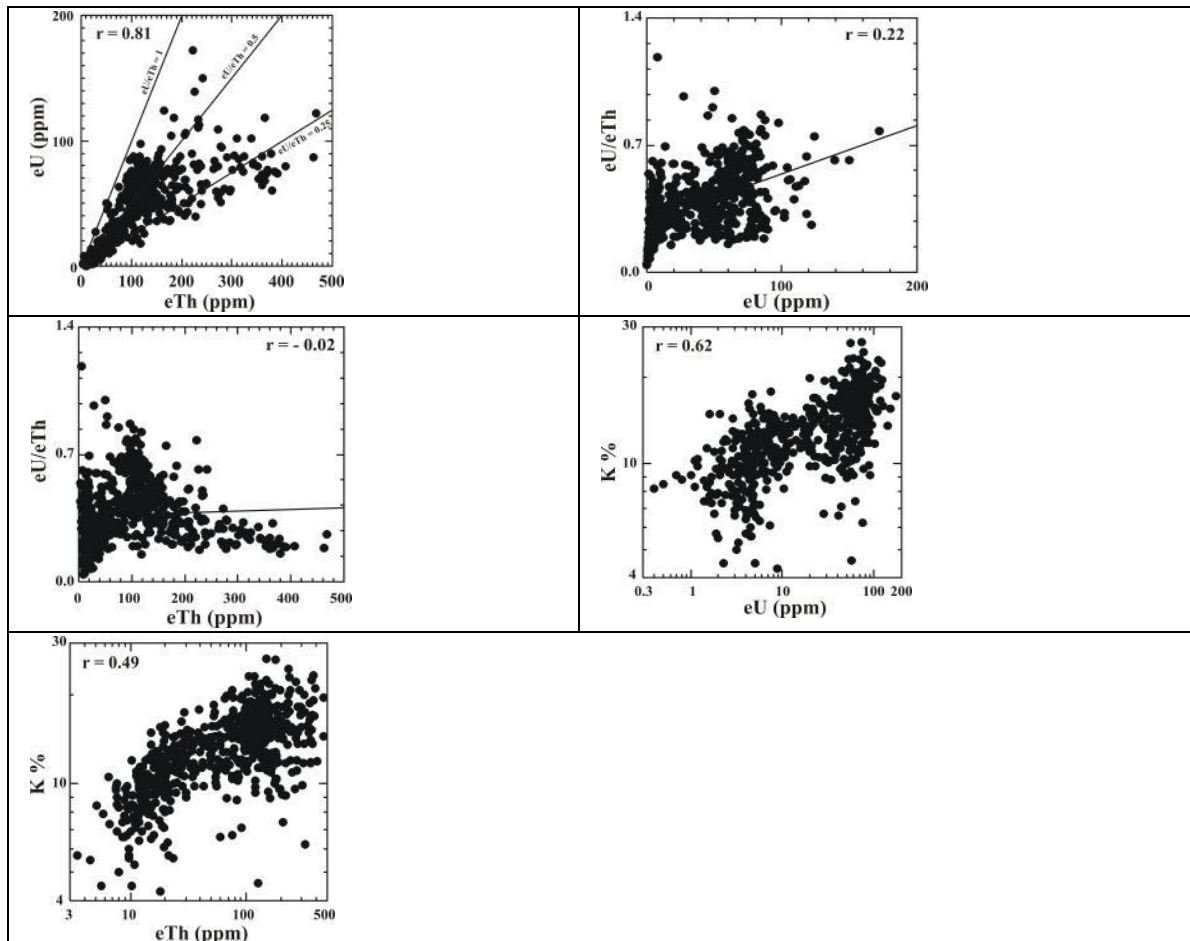


Fig.12 The relation between a) eU-eTh, b) eU-eU/eTh, c) eTh-eU/eTh, d) K-eU and e) K-eTh for studied shear zone I, mylonitic rocks and lamprophyre dykes of Abu Rusheid - Sikait area, SED, Egypt.

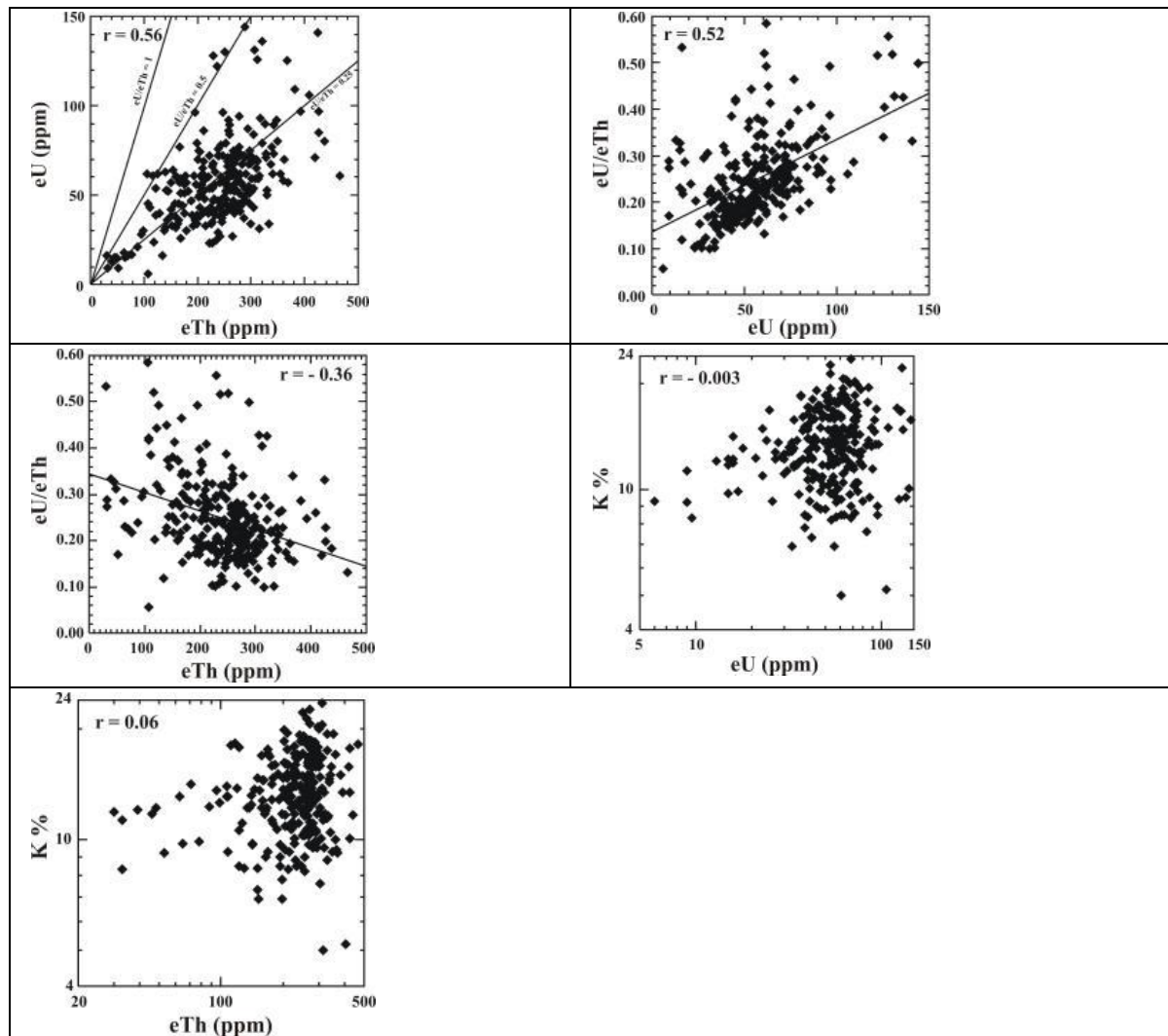


Fig.13 The relation between a) $eU-eTh$, b) $eU-eU/eTh$, c) $eTh-eU/eTh$, d) $K-eU$ and e) $K-eTh$ for studied shear zone II, mylonitic rocks and lamprophyre dykes of Abu Rusheid - Sikait area, SED, Egypt.

6. CONCLUSIONS

The Wadi Abu Rusheid - Sikait area is dissected by NNW-SSE and ENE-WSW shear zones. The surrounding area of lamprophyre dykes comprises, ophiolitic mélange, cataclastic (mylonitic) rocks, granitic rocks and post granitic basic dykes. The cataclastic (mylonitic) rocks are fine to medium - grained and well-banded. The lamprophyre dyke is discontinuous and displaced laterally by numerous strike slip faults (sinistral and dextral). The lamprophyre dyke is composed mainly of plagioclases phenocrysts embedded in fine-grained groundmass of plagioclase, ferromagnesian minerals and quartz. U-minerals (kasolite), apatite and opaques, are accessory. The cataclastic (mylonitic) rock consists essentially of quartz, K-feldspars, plagioclases, biotite and muscovite. Zircon, xenotime, monazite, allanite, fluorite and opaques are accessories.

The mineralizations of the lamprophyre dykes at the studied areas can be classified on basis of mode of occurrence and lithological associations into: -1) Uranium minerals (kasolite), 2) Base metals minerals (sphalerite - cerussite) and 3) REEs and Niobium - Tantalum bearing minerals (xenotime - monazite - tantalite - fergusonite - allanite - apatite - zircon).

Geochemically, the trace and REE elements distribution in the studied lamprophyres are anomalous concentrations; U (4%), Pb (44%), Cu (8%), Y (16%), Rb (3%), Zn (21%) and Zr (3%), La (7%), Ce (6%), Gd (4%), Er (18%), Dy (17%), Nd (11%), Yb (17%) and Sm (5%). The studied lamprophyre dykes are characterized by anomalously high REEs contents ranging from 1035 to 3980 ppm. The LRREs are about 200 to 1000 times the normalized chondritic values while the HREEs recorded

values about 700 to 5000 times compared to the reference chondrite (HREEs>LREEs). The depleted pattern in the shear zones, may due to the hydrothermal solution.

Radiometrically, there are relatively positive relation between eU vs. eTh, slightly strong positive relation between eU vs. K%, eU vs. eU/eTh and weakly positive relation between eTh vs. K%. These positive values of eU indicating the migration of uranium and redeposit in lamprophyre dykes and leading to the enrichment of uranium in lamprophyre dykes from surrounding rocks and enrichment in uranium which related to post-magmatic processes.

ACKNOWLEDGMENTS

The authors would like to thank the all my colleagues of the Radioactive Granitic Department (Nuclear Materials Authority) and Abu Rusheid project (2010-2013) for their help during the work and Dr. Reda El Arafy who kindly made available facilities.

REFERENCES

- [1] **Assaf, H.S., Ibrahim, M.E., Zalata, A.A., Metwally, A.A., and Saleh, G.M. (2000):** Polyphase folding in Nugrus-Sikeit area South Eastern Desert, Egypt. JKAU: Earth Sci., 12, p.1-16.
- [2] **Attawiya, M. Y., El-Mezeyen, A. M., Hassan, M .M., Hashad, A. H., and Ammar, F.A., (1989):** On the metamorphism of the gneisses and metasediments, in South Eastern Desert, Egypt. Bull. Fac., Sci., Zagazig Univ., 11, p.194 - 224.
- [3] **Boynton, W. V. (1984):** Geochemistry of the rare earth elements : meteorite studies. In rare earth element geochemistry (Henderson, P. Ed.). Elsevier, Amesterdam, p.63 -114.
- [4] **Cambon, A. R. (1994):** Uranium deposits in granitic rocks. Notes on the national training course on uranium geology and exploration. Organized by IAEA, p. 8 - 20.
- [5] **Dawoud, M., (2004):** The nature and origin of U-bearing fluids as revealed from zircon alteration: examples from the Gattarian granites of Egypt. Sixth Intern. Conf. Geochem., Alex. Univ., V. I-B, p. 875-891.
- [6] **Deer, W. A., Howie, R. A., and Zussman, J. (1992):** An introduction to the rock forming minerals. Longman group limited, England. Second edition. 696 pp.
- [7] **El Bayoumi, R. M. A., (1984):** Ophiolites and mélange complex of Wadi Ghadir, Eastern Desert, Egypt. Bull. Fac. Earth Sci., King Abdul-Aziz Univ., Jeddah, 6, p.324-329.
- [8] **El Ghazalawi W. S. (2009):** Structural setting and tectonic environment of nugrus-sikait area, south eastern desert, egypt: implication on mineralization. Departement of Geology, Faculty of Science, Suez Canal University, 217 pp.
- [9] **Fowler, A., and Osman A. F., (2009):** The Sha'it–Nugrus shear zone separating Central and South Eastern Deserts, Egypt: A post-arc collision low-angle normal ductile shear zone. J. African Earth Sci., 53, p.16-32.
- [10] **Fielding, P. E. (1970):** The distribution of uranium, rare earths, and color centers in a crystal of natural zircon. The American Mineralogist, Vol.55, March_April, p. 428 - 440.
- [11] **Fritz, H., Wallbrecher, E., Khudeir, A. A., Abu El-Ela, F. F., and Dallmeyer, D. R., (1996):** Formation of Neoproterozoic metamorphic core complexes during oblique convergence Eastern Desert, Egypt. J. African Earth Sci., 23, p.311-329.
- [12] **Greiling, R. O., Kröner, A., El-Ramly, M. F., and Rashwan, A. A., (1988):** Structural relations between the southern and central parts of the Eastern Desert of Egypt: details of an fold and thrusts belt. In: El-Gaby, S., Greiling, R. (Eds.), The Pan-African Belt of the NE Africa and Adjacent Areas. Tectonic Evolution and Economic Aspects. Freidr. Vieweg & Sohn, Braunschweig/Weisbaden, p.121-145.
- [13] **Hassan, M. A.(1964):** Geology and petrographical studies of the radioactive minerals and rocks in Wadi Sikait-Wadi El Gemal area. Eastern Desert, U. A. R: M. Sc. Thesis faculty of science, Cairo Univ. 165pp.
- [14] **Hassan, M. A. (1973):** Geology and geochemistry of radioactive columbite- bearing psammitic gneiss of Wadi Abu Rusheid. South Eastern Desert, Egypte. Annals of Geol. Surv. Egypt. V. III, p.207-225.
- [15] **Hassan, M. A., Aly, M. M. and Eid, A. S. (1983):** Petrographical and geochemical studies on the radioactive psammitic gneiss of Wadi Abu Rusheid, Eastern Desert, Egypt, Annals of the Geol. Surv. of Egypt. V. XIII, p.143-155.

- [16] **Heinrich, E. W. (1962):** Mineralogy and geology of radioactive raw materials. Mc Graw-Hill Book Company, New York.348 pp.
- [17] **Hedenquist, J.W., Izawa, E., Arribas, A., and White, N.C. (1995):** Epithermal gold deposits : Styles ,characteristics and exploration. Resource Geology No. 1, Tokyo. P.172-184.
- [18] **Hitzman et. al. (2003):** Classification, genesis, exploration guides for non sulfide zinc deposits. Economic geology, Vol.98, 2003, p.685-714.
- [19] **Huyneq A. M., Piret-Meunier, J., and Van Meerssche, M. (1963):** Structure de la kasolite. Bulletin De La Classe Des Sciences. Academie Royale De Belgique, 49, p. 192 - 201.
- [20] **Ibrahim, M.A., Amer, T.E., and Saleh, G.M. (1999):** New occurrence of some nuclear materials and gold mineralization at Wadi Sikeit area, South Eastern Desert, Egypt. First seminar on nuclear raw materials and their technology, Cairo, Egypt, p.1-3.
- [21] **Ibrahim, M.A., Saleh, G.M., Ibrahim, H.I., Azab, M.S., Oraby, F., Abu El Hassan, E., Rashed, M.A., and others (2004):** Geology and rare-metal mineralizations of Abu Rusheid shear zone. (Internal report part-2), 155pp.
- [22] **Ibrahim, M. E., El Tokhi, M. M., Saleh, G. M. and Rashed, M. A. (2006);** Lamprophyre bearing REEs,south Eeastern Desert, Egypt.The seventh Inter. Conf. on Geochemistry, p.1-10.
- [23] **Ibrahim, M. E., Saleh, G. M., Dawood, N. A., and Aly, G. A. (2010):** Ocellar lamprophyre dyke bearing mineralization, Wadi Nugrus, Eastern Desert, Egypt: Geology, mineralogy and geochemical implications. Journal of Geology and Mining Research Vol. 2 (4), p. 74 - 86.
- [24] **Kerr, P. F. (1977):** Optical mineralogy. 4th Ed., McGraw-Hill Book Inc., 492 pp.
- [25] **Lightfoot, P.C., (1993):** The interpretation of geoanalytical data, in: Riddle, C. (Ed.), Analysis of Geological Materials. Marcel Dekker Inc., New York, p. 377– 455.
- [26] **McDonough, W. F., Sun, S. S., Ringwood, A. E., Jagoutz, E., and Hofmann, A. W. (1992):** Potassium, rubidium and cesium in the Earth and Moon and the evolution of the mantle of the Earth. Geochim. Cosmochim Acta. 56. p. 1001 - 1012.
- [27] **Myron G. (2003):** Igneous and Metamorphic Petrology. (Second Edition). Blackwell Publishing company, 729pp.
- [28] **Pearce, J.A., (1983):** Role of the sub-continental lithosphere in magma genesis at acrive continental margins, in: Hawkesworth, C.J., Norry, M.J. (Eds.), Continental Basalts and Mantle Xenoliths. Shiva Publishing Ltd., Cambridge, p. 230-249.
- [29] **Palache, C., Berman, H., and Ferondei, C. (1951):** The System of Mineralogy of the Danas, Vo1, 2. John Wiley and Sons, New York.289 pp.
- [30] **Pupin, J. P., and Turcon, G. (1975):** Typologie du zircon accessorie dans les rpches plutoniques dioritiques granitiques et syeritiques, facteurs qssqntiels detedminatles variations typologiques. *Petrologie*, 1 (2). p. 139 - 156.
- [31] **Reynolds, A.N., Sangster, F.D., Allen, R.C., and Carman, E.C. (2003):** Classification, genesis and exploration guides for nonsulfide zinc deposits. Economic Geology, 98, p.685-714.
- [32] **Rose, A.W., Hawkes, H.E., and Webb, J.S. (1979):** Geochemistry in mineral exploration. London, Academic Press, 657pp.
- [33] **Rollinson H. R. (1993):** Using geochemical data: evaluation, presentation, interpretation. Longman Group, UK.197pp.
- [34] **Saleh, G.M. (1997):** The potentiality of uranium occurrences in Wadi Nugrus area, Southeastern Desert, Egypt. Ph.D. Thesis, El Mansoura Univ., 171pp.
- [35] **Saleh, G. M., Mostafa, M. S., Ibrahim, I. H., Mahmoud, F. O., Abu El Hassan, A. A., Rashed, M. A., Khalel, F. M., Mahmoud, M. A., Salem, M. S., Saleh, S. M., and others, (2012):** Uranium mineralization and estimation of mineral resources in the cataclastic rocks of Abu Rusheid area, South Eastern Desert, Egypt. (Internal report). 145 pp.
- [36] **Sangameshwar, S.R., and Barnes, H.L. (1983):** Supergene processes in zinc-lead-silver sulfide ores in carbonate rocks. Economic Geology, 78, p.1379-1397.
- [37] **Stern, R. J. and Hedge, C. E., (1985):** Geochronologic and isotopic constrains on late Precambrian crustal evolution in the Eastern Desert of Egypt, Am. J. Sci., 285, p.97-127.
- [38] **Sun S. S., and McDonough W. F. (1989):** Chemical and isotopic systematics of oceanic basalts: implications for mantle composition and processes. In: Saunders AD, Norry (eds) Magmatism in the ocean basins, v. 42. The Geological Society, London, p. 313-345.

- [39] **Surour, A. A., (1995):** Medium to high - pressure garnet-amphibolites from Gebel Zabara and Wadi Sikeit, South Eastern Desert, Egypt. *J. Earth Sci.*, 21 No. 3, p.434 - 457.
- [40] **Smith, R.L. (1979):** Ash flow magmatism. *Geol. Soc. Amer. Spec. Paper* 180, p.5-27.
- [41] **Vavra, G. (1990):** On the kinematics of zircon growth and its petrogenetic significance: a cathodoluminescent study. *Contribution to Mineralogy and Petrology*, 106. p. 90 - 99.

Citation: *Gehad M. Saleh et.al, (2018). Lamprophyres from Abu Rusheid-Sikait Area, South Eastern Desert, Egypt: Rare Earth Elements, Mineralization and Spectrometric Prospecting, International Journal of Mining Science (IJMS), 4(1), pp.46-59, DOI: <http://dx.doi.org/10.20431/2454-9460.0401004>*

Copyright: © 2018 Gehad M. Saleh. This is an open-access article distributed under the terms of the Creative Commons Attribution License, which permits unrestricted use, distribution, and reproduction in any medium, provided the original author and source are credited